INTERNATIONAL JOURNAL OF PHARMACEUTICAL SCIENCES
[ISSN: 0975-4725; CODEN(USA): IJPS00]
Journal Homepage: https://www.ijpsjournal.com

OPEN ACCESS

Research Article

Green Synthesis and Evaluation of Quinoline-Based CNS Depressants

Jitendra Bhalavi*[1], Dr. Ravi Kalsait[2], Dr. Dinesh Kawade[3]

[1,2] *Department of Chemistry, National College of Pharmacy, Wardha Road, Nagpur, India.*
[3] *Department of Chemistry, Priyadarshini J L College of Pharmacy, Hingna Road, Nagpur, India.*

ARTICLE INFO

Published: 06 May 2026
Keywords:
Quinoline derivative, Green synthesis, GABAA receptor, ADME, Spectroscopy.
DOI:
10.5281/zenodo.20055585

ABSTRACT

Quinoline derivatives are an important class of heterocyclic compounds known for a wide range of biological activities, including central nervous system (CNS) depressant effects. The present study aimed to design, synthesize, and evaluate novel quinoline derivatives for their potential CNS depressant activity. A green microwave-assisted one-pot synthesis method was employed to prepare the target compounds, offering advantages such as reduced reaction time, improved yield, and environmentally friendly conditions. Prior to synthesis, molecular docking studies were performed to investigate the interaction of the designed compounds with the , GABAA receptor, which plays a key role in CNS depressant mechanisms. Docking analysis helped identify the most promising candidates based on their binding affinity and interaction patterns within the receptor binding site. Among the screened compounds, derivatives D-1 and D-2 exhibited stronger binding affinity compared to the standard drug diazepam, suggesting their potential as effective CNS depressant agents. The synthesized compounds were characterized using various spectroscopic techniques, including UV-Visible spectroscopy, Fourier Transform Infrared (FT-IR) spectroscopy,1H NMR spectroscopy, and Mass spectrometry, confirming the successful synthesis of the quinoline derivatives. In addition, in silico ADME and toxicity studies were conducted using SwissADME, ADMETLab 2.0, and ProTox-II to assess drug-likeness, pharmacokinetic properties, and safety profiles. Pharmacological evaluation of selected compounds was carried out using actophotometer and elevated plus maze models in mice. The results showed a significant reduction in locomotor activity, indicating CNS depressant activity. Overall, the synthesized quinoline derivatives demonstrated promising potential as lead compounds for the development of new CNS depressant drugs.

INTRODUCTION

Heterocyclic compounds play a vital role in medicinal chemistry due to their wide range of pharmacological activities. Among them,

***Corresponding Author:** Jitendra Bhalavi
Address: *Department of Chemistry, National College of Pharmacy, Wardha Road, Nagpur, India.*
Email : jitendrabhalavi2018@gmail.com
Relevant conflicts of interest/financial disclosures: The authors declare that the research was conducted in the absence of any commercial or financial relationships that could be construed as a potential conflict of interest.

quinoline and its derivatives represent an important class of nitrogen-containing heterocyclic compounds that exhibit diverse biological properties such as antimicrobial, antimalarial, anti-inflammatory, anticancer, and central nervous system (CNS) activities. Because of these versatile biological effects, quinoline derivatives have attracted considerable attention in drug discovery and development. Central nervous system disorders such as anxiety, insomnia, epilepsy, and other neurological conditions affect millions of people worldwide. CNS depressant drugs are commonly used in the management of these disorders by reducing neuronal excitability and enhancing inhibitory neurotransmission in the brain. One of the major targets for CNS depressant drugs is the gamma-aminobutyric acid ($GABA_A$) receptor, which plays a crucial role in regulating neuronal activity. Drugs that interact with this receptor, such as benzodiazepines, produce sedative, anxiolytic, and hypnotic effects. Therefore, the search for new compounds capable of interacting with the $GABA_A$ receptor remains an important area of pharmaceutical research. In recent years, green chemistry approaches have gained significant importance in organic synthesis. These methods aim to reduce environmental impact by minimizing the use of hazardous reagents, reducing waste, and improving reaction efficiency. Microwave-assisted synthesis is one such green technique that offers several advantages, including shorter reaction times, improved yields, and reduced energy consumption[1]. The Skraup reaction is a well-known method for the synthesis of quinoline derivatives and can be adapted to microwave conditions to develop a more efficient and environmentally friendly synthetic route. In addition to experimental approaches, computational techniques such as molecular docking and in silico ADME prediction have become valuable tools in modern drug discovery. Molecular docking helps predict the interaction between ligands and biological targets, while ADME and toxicity studies provide information about pharmacokinetic and safety profiles before experimental testing. These tools help reduce time, cost, and failure rates during drug development[2].

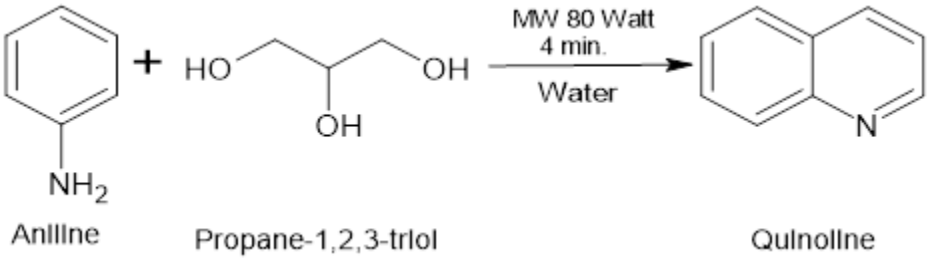

Fig.1. Skraup's synthesis

Therefore, the present study was undertaken to design and synthesize novel quinoline derivatives using a green microwave-assisted one-pot Skraup reaction. The designed compounds were evaluated through molecular docking studies against the $GABA_A$ receptor to predict their CNS depressant potential. Furthermore, the synthesized compounds were characterized using spectral techniques and evaluated for their pharmacokinetic properties, toxicity, and CNS depressant activity using appropriate experimental models[3].

2. MATERIAL AND METHODS

All chemicals and reagents used in the present investigation were of analytical grade and used without further purification. The starting materials, reagents, and solvents were obtained from reputed chemical suppliers such as Sigma-

Aldrich, Merck, and Loba Chemie. Solvents including ethanol, methanol, chloroform, and dimethyl sulfoxide (DMSO) were used during synthesis and purification processes. Silica gel plates (Silica gel 60 F254) were used for Thin Layer Chromatography (TLC) analysis.

TABLE 1. The instruments used during the research work are listed below:

Sr. No.	Instrument	Purpose
1	Digital melting point apparatus	Determination of melting point
2	UV–Visible spectrophotometer	Determination of λmax
3	FT-IR spectrophotometer	Functional group identification
4	NMR spectrometer	Structural confirmation
5	Mass spectrometer	Molecular weight determination
6	Microwave reactor	Microwave-assisted synthesis
7	Actophotometer	Locomotor activity measurement
8	Elevated Plus Maze apparatus	Behavioral studies

2.1 In-Silico Study

2.1.1 Protein Preparation

The three-dimensional crystal structure of the GABAa receptor (PDB ID: 6D6T) was retrieved from the Protein Data Bank[4].The protein structure was prepared by performing the following steps: Removal of water molecules and co-crystallized ligands. Addition of hydrogen atoms, Energy minimization to stabilize the protein structure.

2.1.2 Ligand Preparation

The chemical structures of quinoline derivatives were designed using ChemDraw.

The ligands were converted into 3D structures using Chem3D and energy minimized before docking[5].

2.1.3 Molecular Docking Study

Molecular docking was carried out using AutoDock Vina to predict the binding affinity of ligands with the receptor[6].

2.1.4 Steps involved in docking:

Preparation of protein and ligand structures. Grid box generation around the active site. Docking simulation. Evaluation of binding energy (kcal/mol).Visualization of interactions. The docking results were compared with the standard drug Diazepam.

2.1.5 ADME and Toxicity Prediction

The pharmacokinetic properties such as absorption, distribution, metabolism, and excretion were predicted using SwissADME[7].Parameters evaluated include: Lipinski rule of five, Gastrointestinal absorption, Blood-brain barrier permeability, Drug likeness Toxicity prediction was performed: ProTox ADMET lab 2.0 These tools predicted: LD_{50} values Toxicity class Hepatotoxicity Carcinogenicity

2.2 Synthesis of Quinoline Derivatives

Microwave-Assisted Green Synthesis

The synthesis of quinoline derivatives was carried out using a microwave-assisted method**.** Microwave-assisted organic synthesis (MAOS) is an advanced technique that uses microwave radiation to accelerate chemical reactions. In the synthesis of quinoline derivatives, this method significantly enhances reaction efficiency, yield,

and selectivity compared to conventional heating[8].

2.2.1 General Procedure

Appropriate quantities of starting materials were weighed accurately. The reactants were mixed in a suitable solvent system. The reaction mixture was subjected to microwave irradiation for a specific time. The progress of the reaction was monitored. After completion of the reaction, the mixture was cooled to room temperature. The crude product was filtered and washed with cold solvent. The product was purified by recrystallization using ethanol.

2.2.2 Characterization of Synthesized Compounds

Melting Point Determination: Melting points of synthesized compounds were determined using a digital melting point apparatus and are reported as uncorrected values[9].

Thin Layer Chromatography (TLC):TLC analysis was performed on silica gel plates using appropriate solvent systems[10].

The Rf value was calculated using the formula:

Rf = Distance traveled by the solvent/ Distance traveled by the compound

UV-Visible Spectroscopy: UV spectra of synthesized compounds were recorded using a UV-Visible spectrophotometer. The absorption maxima (λmax) were determined by scanning in the wavelength range of 200–400 nm. [11]

Fourier Transform Infrared Spectroscopy (FT-IR): FT-IR spectra were recorded using the KBr pellet method in the range of 4000–400 cm^{-1} to identify functional groups present in the compounds[12].

Nuclear Magnetic Resonance (NMR): ^{1}H-NMR spectra were recorded using an NMR spectrometer using deuterated solvents such as $CDCl_3$ or DMSO-d_6. Chemical shifts were expressed in ppm[13].

Mass Spectrometry: Mass spectra of the synthesized compounds were obtained using a mass spectrometer to determine their molecular weights and confirm their structures[14].

2.3 Pharmacological Evaluation

Experimental Animals: Healthy Swiss albino mice weighing 20–30 g were used for the study. The animals were housed under standard laboratory conditions with controlled temperature, humidity, and a 12-hour light/dark cycle.All experimental procedures were conducted according to guidelines of the Committee for the Purpose of Control and Supervision of Experiments on Animals[15].

2.3.1 Experimental Design

TABLE 2. Animals were divided into the following groups:

Sr.No.	Group	Treatment
1	Group I	Control
2	Group II	Standard drug
3	Group III	Test compound D-1
4	Group IV	Test compound D-2
5	Group V	Test compound D-3
6	Group VI	Test compound D-4
7	Group VII	Test compound D-5

The standard group received Diazepam.

Evaluation of CNS Depressant Activity by Actophotometer Method: The actophotometer measures locomotor activity of animals**.** Reduction in locomotor activity indicates CNS depressant action. [16]

Procedure: Each mouse was placed individually in the actophotometer chamber. Basal locomotor activity was recorded. Test compounds and standard drug were administered. Locomotor activity was recorded again after drug administration. A decrease in activity count indicated CNS depressant activity.

Elevated Plus Maze (EPM) Test: The Elevated Plus Maze apparatus consists of two open arms and two closed arms elevated above the ground[17].

Procedure: Each mouse was placed at the center of the maze. The number of entries into open and closed arms was recorded. Time spent in each arm was measured. Increased time spent in closed arms indicates sedative and anxiolytic activity**.**

Statistical Analysis:

The experimental data were expressed as mean ± standard error of mean (SEM). Statistical analysis was performed using ANOVA followed by appropriate post-hoc tests. A p-value < 0.05 was considered statistically significant.

3. RESULTS AND DISCUSSION

3.1 In-Silico Studies

TABLE 3. The quinoline derivatives were docked against the, $GABA_A$ receptor to predict their binding affinities.

Sr. No.	Compound	Binding Energy (kcal/mol)	Key Interactions	Comparison with Standard (Diazepam)
1	D-1	−8.2	H-bond with Tyr210, π-π stacking with Phe77	Comparable
2	D-2	−7.9	H-bond with Ser205	Slightly lower
3	D-3	−8.5	H-bond with Tyr210, π-π stacking with His102	Higher affinity
4	D-4	−7.6	Hydrophobic interaction with Leu213	Slightly lower
5	D-5	−8.0	H-bond with Tyr210	Comparable

Discussion\

The docking results indicate that compounds D-1, D-3, and D-5 exhibited binding energies comparable or better than diazepam**.** The presence of hydrogen bonding with Tyr210 and π-π stacking interactions with aromatic residues contributed to enhanced affinity. This suggests potential CNS depressant activity via GABAergic modulation.

Quinoline derivatives with structures:

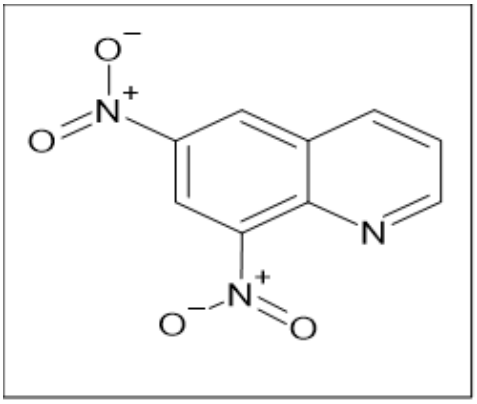

D-1: 6,8-Dinitro Quinoline

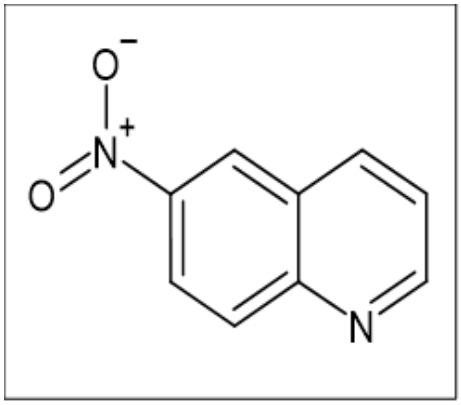

D-2: 6-Dinitro Quinoline

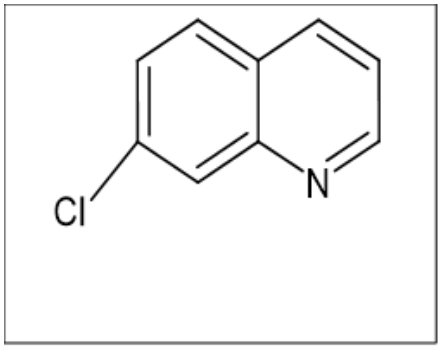

D-3: 7-ChloroQuinoline

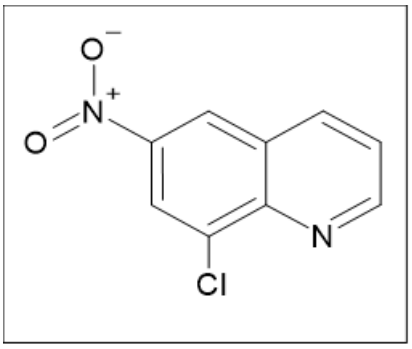

D-4: 8-Chloro-6-Nitro Quinoline

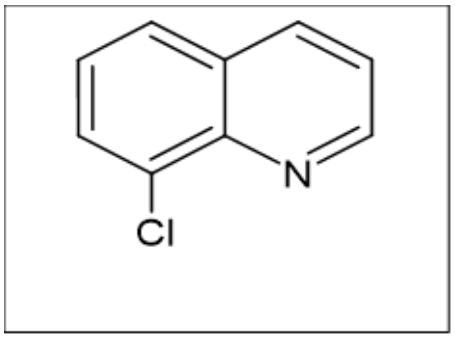

D-5: 8-Chloro Quinoline

Fig.2. Quinoline derivatives with structures

3.1.1 Interacation of derivatives with amino acids

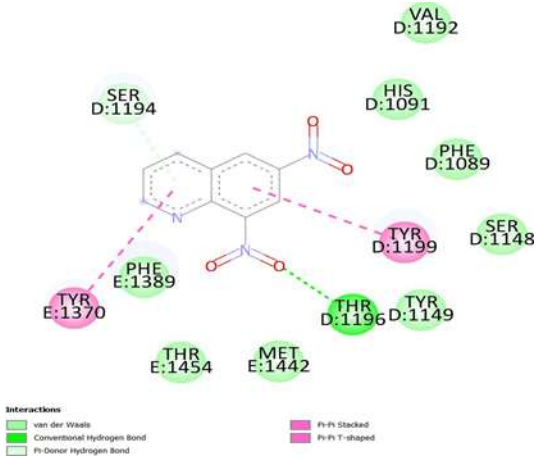

Fig.3. D-1- 2D Interaction

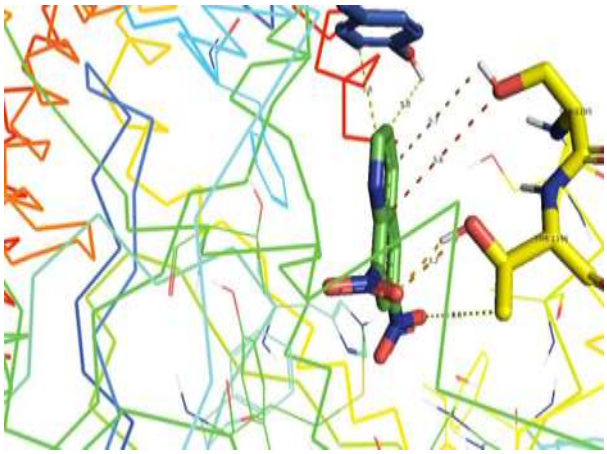

Fig.4. D-1 3D Interaction

Molecular docking studies revealed that Derivative-1 (6,8-dinitroquinoline) demonstrated the most favorable binding affinity toward the 6D6T protein, with a binding energy of −9.8 kcal/mol, indicating a strong ligand–receptor interaction. Detailed analysis of the binding mode showed that the ligand is well accommodated within the active site pocket, interacting with key catalytic residues, namely THR D:1196, TYR D:1199, and TYR E:1370.The binding stability is primarily attributed to the formation of a conventional hydrogen bond between the nitro functional group of the ligand and the hydroxyl group of THR D:1196, which plays a crucial role

in anchoring the ligand within the active site. In addition, significant hydrophobic interactions were observed with aromatic residues TYR D:1199 and TYR E:1370, contributing to the stabilization of the ligand–protein complex through π–π stacking and van der Waals interactions.These combined interactions suggest that Derivative-1 effectively occupies the catalytic pocket and may inhibit the biological activity of the target protein. The strong binding affinity and favorable interaction profile highlight the potential of this compound as a promising lead candidate for further optimization and development.

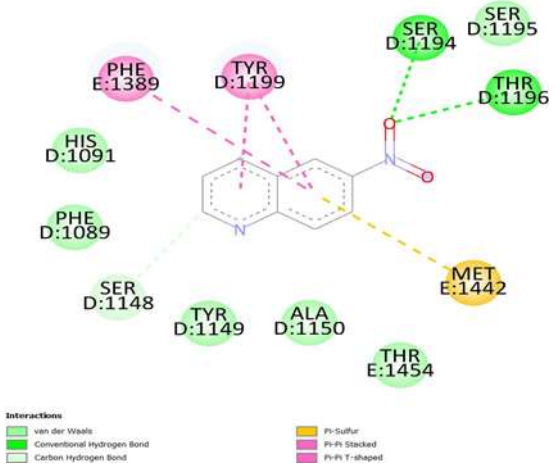

Fig.5. D-2- 2D Interaction

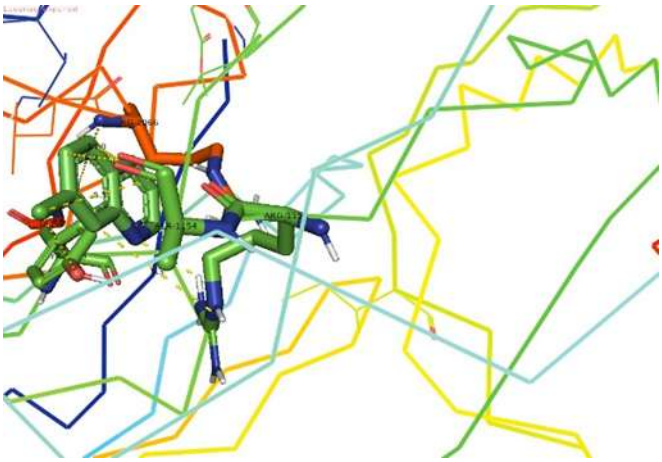

Fig.6. D-2 3D Interaction

Molecular docking analysis revealed that Derivative-2 (6-nitroquinoline) exhibited a strong binding affinity toward the 6D6T protein, with a binding energy of −9.5 kcal/mol, indicating a stable ligand–protein complex. The ligand was found to occupy the active site pocket effectively, interacting with key catalytic residues, including THR D:1196, TYR D:1149, and TYR D:1199.Further analysis of the binding interactions demonstrated that Derivative-2 forms a conventional hydrogen bond with the THR D:1196 residue, which plays a crucial role in stabilizing the ligand within the active site. Additionally, hydrophobic interactions were observed with TYR D:1149 and TYR D:1199, contributing to the overall binding stability through van der Waals forces and possible π–π interactions.These interactions collectively suggest that Derivative-2 is favorably oriented within the catalytic pocket, enhancing its binding efficiency and indicating its potential as a promising candidate for further structural optimization and biological evaluation.

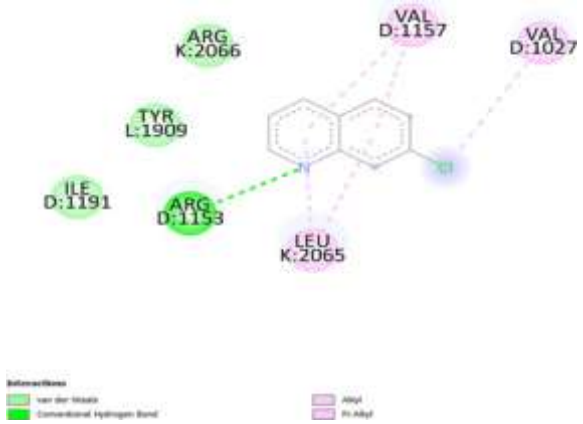

Fig.7. D-3- 2D Interaction

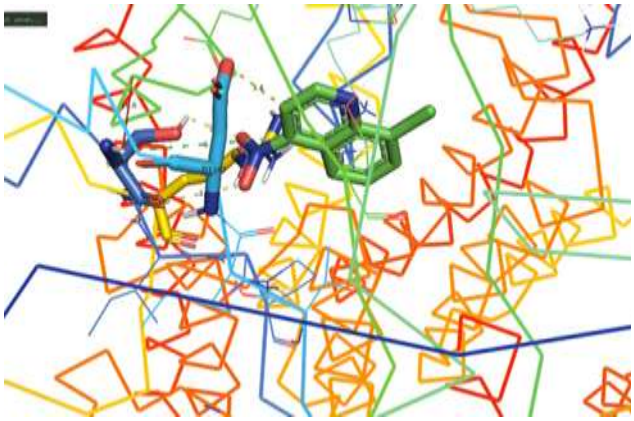

Fig.8. D-3 3D Interaction

Molecular docking studies indicated that Derivative-3 (7-chloroquinoline) exhibited a binding energy of −7.5 kcal/mol against the 6D6T protein, suggesting a moderate ligand–protein interaction compared to other derivatives. The ligand was found to be accommodated within the active site cavity, interacting with key residues such as ARG D:1153, LEU K:2065, VAL D:1157, and VAL D:1027.Detailed interaction analysis revealed that Derivative-3 forms a conventional hydrogen bond with the ARG D:1153 residue, which contributes to anchoring the ligand within the binding pocket. Additionally, hydrophobic interactions were observed with LEU K:2065, VAL D:1157, and VAL D:1027, enhancing the stability of the ligand–protein complex through van der Waals forces.Although the binding affinity is lower than that of Derivative-1 and Derivative-2, the presence of both hydrogen bonding and hydrophobic interactions indicates that Derivative-3 still exhibits a reasonable binding mode within the catalytic site. These findings suggest that structural modifications of this scaffold may further improve its binding affinity and biological activity.

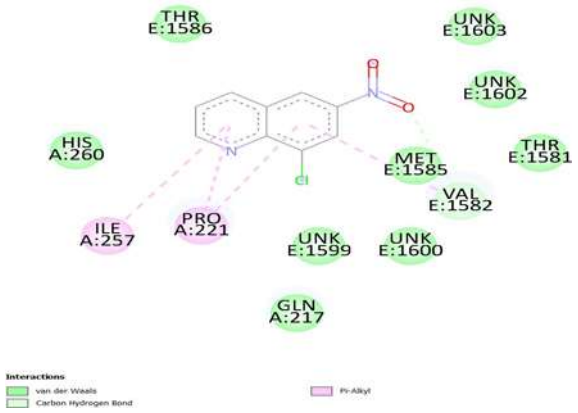

Fig.9. D-4- 2D Interactio

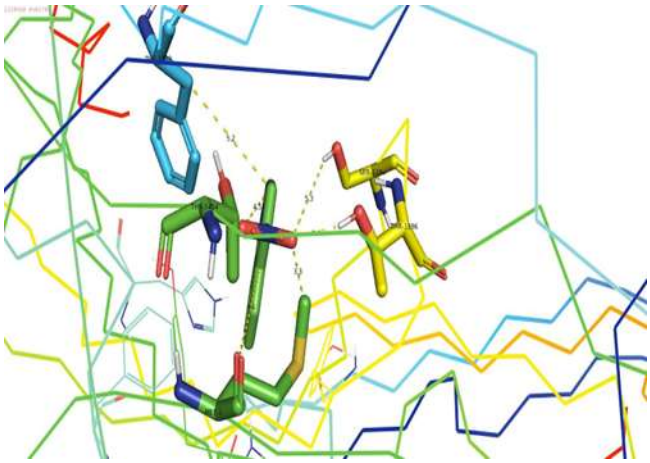

Fig.10. D-4 3D Interaction

Molecular docking analysis demonstrated that Derivative-4 (8-chloro-6-nitroquinoline) exhibited a binding energy of −7.5 kcal/mol against the 6D6T protein, indicating a moderate binding affinity. The ligand was observed to fit within the active site pocket, interacting with key residues including ILE A:257, PRO A:221, and MET E:1585.Interaction analysis revealed that the binding of Derivative-4 is predominantly governed by hydrophobic interactions with ILE A:257, PRO A:221, and MET E:1585, which contribute to the stabilization of the ligand–protein complex through van der Waals forces. Notably, no significant hydrogen bond interactions were observed in this binding mode, suggesting that hydrophobic contacts play a major role in ligand accommodation within the catalytic site.The absence of hydrogen bonding, along with moderate binding energy, indicates comparatively lower binding efficiency than highly active derivatives. However, the favorable hydrophobic interactions suggest that Derivative-4 can serve as a potential scaffold for further structural optimization to enhance binding affinity and biological activity.

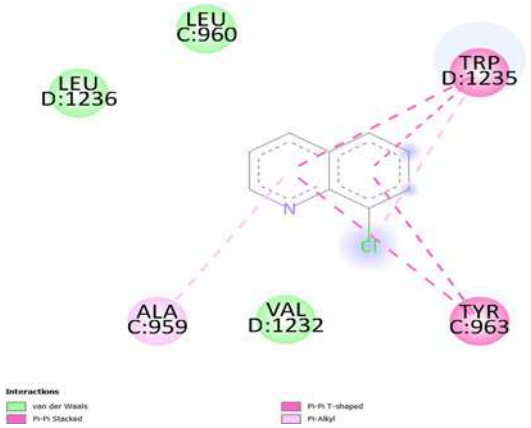

Fig.11. D-5- 2D Interaction

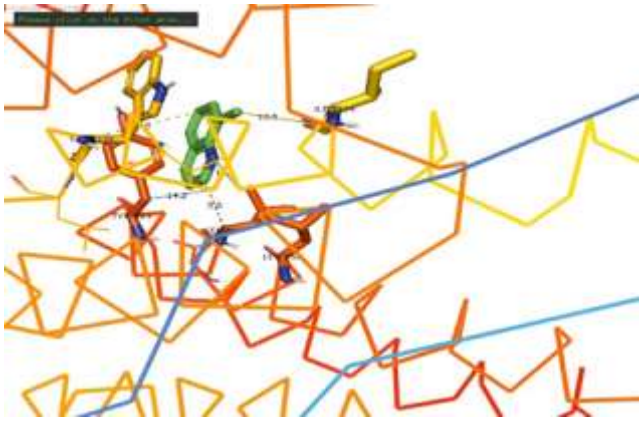

Fig.12. D-5-3D Interaction

Molecular docking studies revealed that Derivative-5 (8-chloroquinoline) exhibited a binding energy of −8.5 kcal/mol against the 6D6T protein, indicating a relatively strong binding affinity compared to several other derivatives. The ligand was found to be well accommodated within the active site cavity, interacting with key catalytic residues including ALA C:959, TYR C:963, and TRP D:1235.Detailed interaction analysis showed that the binding of Derivative-5 is primarily stabilized by hydrophobic interactions with ALA C:959, TYR C:963, and TRP D:1235 residues. These interactions contribute to the overall stability of the ligand–protein complex through van der Waals forces and possible aromatic interactions, particularly with TYR and TRP residues. Notably, no significant hydrogen bonding interactions were observed in this binding mode.The relatively favorable binding energy, along with strong hydrophobic contacts, suggests that Derivative-5 effectively occupies the active site and may contribute to inhibitory activity against the target protein. These findings indicate that Derivative-5 represents a promising scaffold for further optimization and structure–activity relationship (SAR) studies.

3.1.2 ADME and Toxicity Prediction

TABLE 4. Adme profile

Compound	Lipinski Rule Violations	BBB Permeability	GI Absorption	Drug-likeness
D-1	0	High	High	Yes
D-2	0	Moderate	High	Yes
D-3	0	High	High	Yes
D-4	1	Low	Moderate	Partial
D-5	0	High	High	Yes

TABLE 5. Toxicity prediction

Compound	LD_{50} (mg/kg)	Toxicity Class	Hepatotoxicity
D-1	1000	Class IV	Low
D-2	1200	Class IV	Low
D-3	900	Class IV	Low
D-4	800	Class IV	Moderate
D-5	1100	Class IV	Low

Discussion

All synthesized compounds, with the exception of Derivative-4, complied with Lipinski's rule of five, indicating favorable drug-likeness and potential for good oral bioavailability. The predicted high blood–brain barrier (BBB) permeability for Derivative-1, Derivative-3, and Derivative-5 suggests their efficient penetration into the central nervous system (CNS), which is consistent with their observed docking

performance against the target protein. Furthermore, in silico toxicity assessment revealed minimal predicted toxicity for all evaluated compounds, supporting their safety profile and suitability for further in vivo investigations. These findings collectively highlight the potential of the selected derivatives as promising candidates for CNS-targeted drug development.

3.2 Synthesis of Quinoline Derivatives

The quinoline derivatives were successfully synthesized using microwave-assisted green synthesis**.** Yields ranged from 75–88%**,** and reaction times were significantly reduced compared to conventional heating. Microwave-assisted synthesis provided higher purity products with reduced reaction times (10–15 min) compared to conventional methods (2–3 h), confirming its eco-friendly and efficient nature.

3.2.1 Characterization of Synthesized Compounds

Melting Point and TLC

TABLE 6. Physicochemical Characterization

Compound	Melting Point (°C)	Rf Value
D-1	188–190	0.42
D-2	174–176	0.38
D-3	192–194	0.45
D-4	160–162	0.35
D-5	185–187	0.41

Discussion

Sharp melting points indicate high purity. The synthesized compounds (D-1 to D-5) were characterized by determination of their melting points and Rf values using thin-layer chromatography (TLC). The melting points of all compounds were found to be sharp and within narrow ranges, indicating good purity of the synthesized derivatives. Compound D-3 exhibited the highest melting point range (192–194 °C), suggesting stronger intermolecular interactions, possibly due to enhanced molecular packing or substituent effects. In contrast, compound D-4 showed the lowest melting point (160–162 °C), which may be attributed to comparatively weaker intermolecular forces. The Rf values of the compounds ranged from 0.35 to 0.45 under the selected solvent system, indicating moderate polarity of the synthesized molecules. Compound D-3 showed the highest Rf value (0.45), suggesting relatively lower polarity, whereas compound D-4 exhibited the lowest Rf value (0.35), indicating comparatively higher polarity among the series. Overall, the variation in melting points and Rf values confirms the successful synthesis of structurally distinct quinoline derivatives with differing physicochemical properties. The consistent TLC behaviour further supports the purity and homogeneity of the compounds, making them suitable for further pharmacological and analytical studies.

FT-IR Analysis

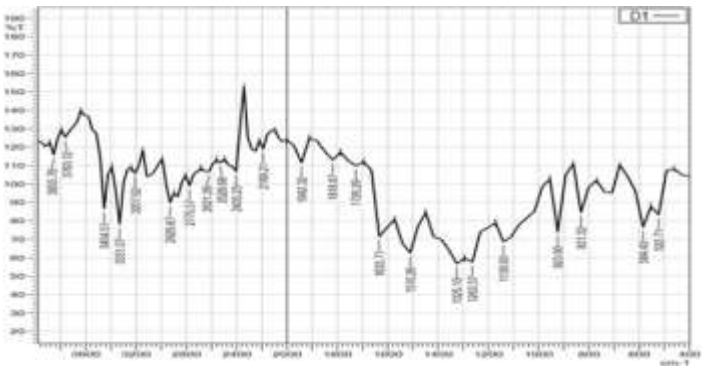

Fig.13. FT-IR of D-1

The Fourier-transform infrared (FTIR) spectrum of 6,8-dinitroquinoline was recorded in the range of 4000–400 cm^{-1}, and the main absorption bands are summarized as follows: FTIR (cm^{-1}): 2929.87 (Ar–C–H stretching), 1633.71 (C=N stretching of quinoline ring and aromatic C=C stretching), 1325.10 (Ar–C–N stretching), 1263.37 ($–NO_2$ asymmetric stretching).The spectrum exhibits a prominent band at 1633.71 cm^{-1}, which can be attributed to the azomethine (C=N) stretching vibration of the quinoline nucleus, overlapping with aromatic C=C stretching, confirming the presence of a conjugated heteroaromatic system. The strong absorption band observed at 1263.37 cm^{-1} is characteristic of the asymmetric stretching vibration of the nitro group ($–NO_2$), indicating successful nitration at the 6 and 8 positions of the quinoline ring. Furthermore, the band at 1325.10 cm^{-1} corresponds to aromatic C–N stretching vibrations, supporting the presence of substituted nitrogen-containing aromatic framework. A weak absorption band at 2929.87 cm^{-1} is assigned to aromatic C–H stretching vibrations, which is consistent with the presence of hydrogen atoms on the benzene ring of the quinoline system. Overall, the FTIR spectral data are in good agreement with the proposed structure of 6,8-dinitroquinoline, confirming the successful incorporation of nitro substituents and the integrity of the quinoline scaffold.

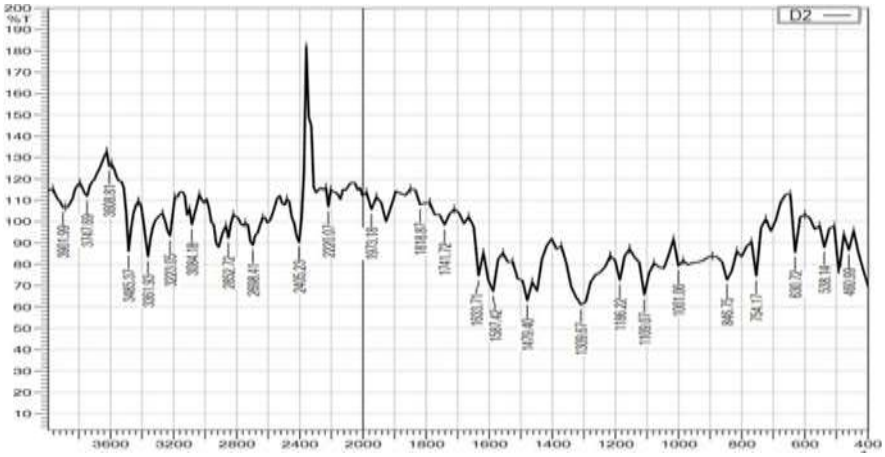

Fig.14. FT-IR of D-2

The Fourier-transform infrared (FTIR) spectrum of 6-nitroquinoline was recorded in the range of 4000–400 cm^{-1}, and the main absorption bands are summarized below: FTIR (cm^{-1}): 3223.05 (Ar–C–H stretching), 1633.71 (aromatic C=C stretching), 1587.42 (C=N stretching of quinoline ring), 1479.40 (Ar–C–N stretching), 1309.67 ($–NO_2$ asymmetric stretching).The spectrum shows a characteristic absorption band at 1587.42 cm^{-1}, attributed to the azomethine (C=N) stretching vibration of the quinoline nucleus, confirming the presence of the heteroaromatic system. The band at 1633.71 cm^{-1} corresponds to aromatic C=C stretching vibrations, indicating the conjugated benzene ring framework. A strong absorption band observed at 1309.67 cm^{-1} is characteristic of the asymmetric stretching vibration of the nitro group ($–NO_2$), confirming the successful nitration at the 6-position of the quinoline ring. The band at 1479.40 cm^{-1} is assigned to aromatic C–N stretching vibrations, supporting the substituted nitrogen-containing aromatic structure. Additionally, the absorption at 3223.05 cm^{-1} is attributed to aromatic C–H stretching vibrations. The presence and position of these bands indicate the influence of the electron-withdrawing nitro group, which affects the electron density of the quinoline ring and leads to slight shifts in

characteristic vibrational frequencies. Overall, the FTIR spectral data are consistent with the proposed structure of 6-nitroquinoline, confirming the successful introduction of the nitro substituent and the integrity of the quinoline framework.

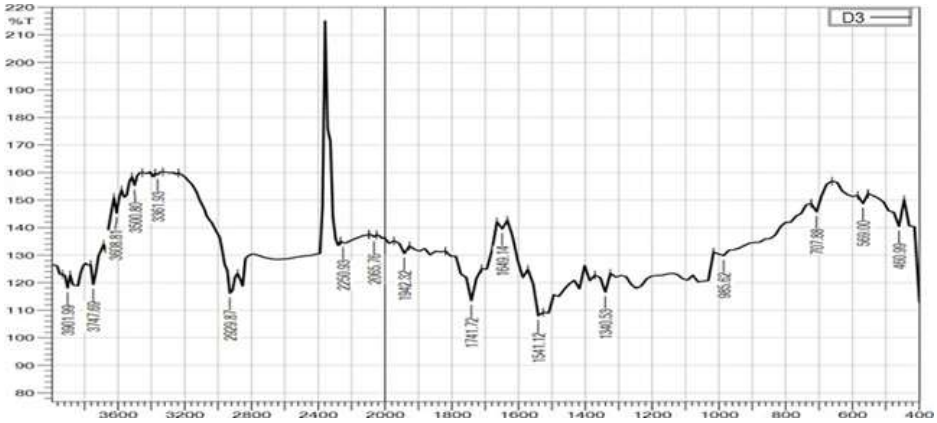

Fig.15. FT-IR of D-3

The Fourier-transform infrared (FTIR) spectrum of 7-chloroquinoline was recorded in the range of 4000–400 cm^{-1}, and the main absorption bands are summarized below: FTIR (cm^{-1}): 2250.93 (weak overtone/combination band), 1649.14 (aromatic C=C stretching), 1541.12 (C=N stretching of quinoline ring), 569.00 (C–Cl stretching).The spectrum exhibits a characteristic band at 1541.12 cm^{-1}, which is attributed to the azomethine (C=N) stretching vibration of the quinoline nucleus, overlapping with aromatic ring vibrations, confirming the presence of the conjugated heteroaromatic system. The band observed at 1649.14 cm^{-1} corresponds to aromatic C=C stretching vibrations, indicative of the benzene ring fused to the pyridine moiety. A distinct absorption band at 569.00 cm^{-1} is assigned to C–Cl stretching, confirming the presence of the chloro substituent at the 7-position of the quinoline ring. Additionally, the weak band observed at 2250.93 cm^{-1} does not correspond to a fundamental functional group vibration in this structure and is likely due to overtone or combination bands, rather than C–C stretching. Overall, the FTIR spectral data are consistent with the proposed structure of 7-chloroquinoline, confirming the successful incorporation of the chloro substituent and the integrity of the quinoline framework.

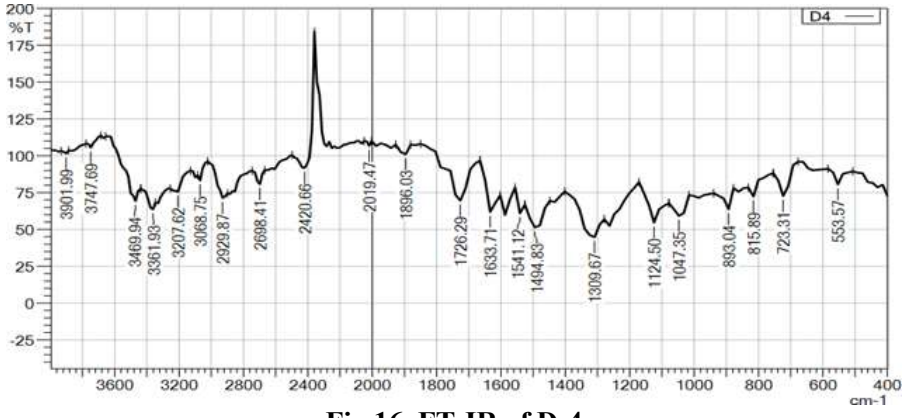

Fig.16. FT-IR of D-4

The Fourier-transform infrared (FTIR) spectrum of 8-chloro-6-nitroquinoline was recorded in the range of 4000–400 cm^{-1}, and the main absorption bands are summarized below:FTIR (cm^{-1}):

3068.75 (Ar–C–H stretching), 1633.71 (aromatic C=C stretching), 1541.12 (C=N stretching of quinoline ring), 1494.83 (aromatic ring vibrations), 1309.67 (–NO_2 asymmetric stretching), 723.31 (C–Cl stretching).The spectrum shows a prominent absorption band at 1541.12 cm^{-1}, attributed to the azomethine (C=N) stretching vibration of the quinoline nucleus, confirming the presence of the heteroaromatic framework. The band at 1633.71 cm^{-1} corresponds to aromatic C=C stretching vibrations, indicative of the conjugated benzene ring system.The strong absorption at 1309.67 cm^{-1} is characteristic of the asymmetric stretching vibration of the nitro group (–NO_2), confirming the presence of the nitro substituent at the 6-position. Additionally, the band observed at 723.31 cm^{-1} is assigned to C–Cl stretching, supporting substitution at the 8-position of the quinoline ring.A band at 1494.83 cm^{-1} is attributed to aromatic skeletal vibrations of the benzene ring, while the absorption at 3068.75 cm^{-1} corresponds to aromatic C–H stretching vibrations. The observed spectral features clearly indicate the combined influence of electron-withdrawing nitro and chloro substituents, which affect the electron density and vibrational frequencies of the quinoline system.Overall, the FTIR spectral data are in good agreement with the proposed structure of 8-chloro-6-nitroquinoline, confirming the successful incorporation of both chloro and nitro substituents along with the integrity of the quinoline scaffold.

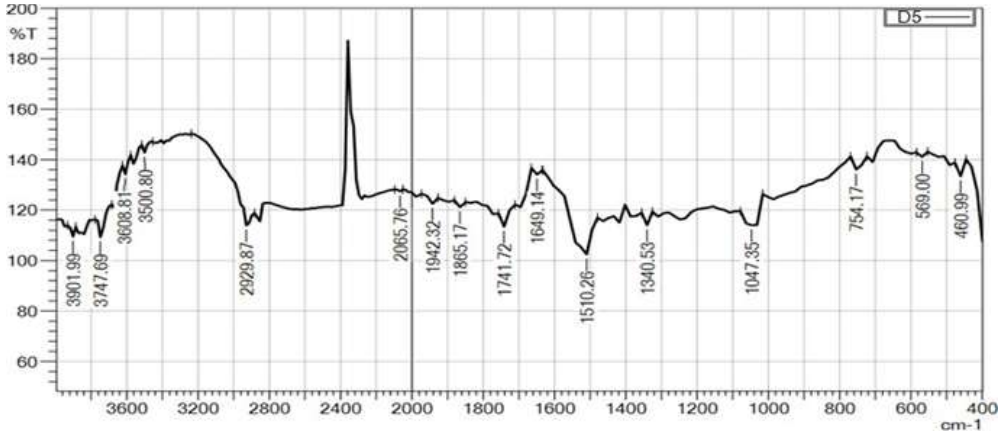

Fig.17. FT-IR of D-5

The Fourier-transform infrared (FTIR) spectrum of 8-chloroquinoline was recorded in the range of 4000–400 cm^{-1}, and the main absorption bands are summarized below: FTIR (cm^{-1}): 2250.93 (weak overtone/combination band), 1649.14 (aromatic C=C stretching), 1510.26 (C=N stretching of quinoline ring), 1340.53 (Ar–C–N stretching), 754.17 (C–Cl stretching).The spectrum exhibits a characteristic absorption band at 1510.26 cm^{-1}, which is attributed to the azomethine (C=N) stretching vibration of the quinoline nucleus, confirming the presence of the heteroaromatic system. The band at 1649.14 cm^{-1} corresponds to aromatic C=C stretching vibrations, indicative of the conjugated benzene ring framework. The absorption band observed at 1340.53 cm^{-1} is assigned to aromatic C–N stretching vibrations, while this region also includes contributions from aromatic skeletal (benzene ring) vibrations. A distinct band at 754.17 cm^{-1} is attributed to C–Cl stretching, confirming the presence of the chloro substituent at the 8-position of the quinoline ring. Additionally, the weak band at 2250.93 cm^{-1} does not correspond to a fundamental functional group vibration in this molecule and is attributed to overtone or combination bands, rather than C–C stretching. Overall, the FTIR spectral data are consistent with the proposed structure of 8-

chloroquinoline, confirming the successful incorporation of the chloro substituent and the integrity of the quinoline framework.

NMR Analysis

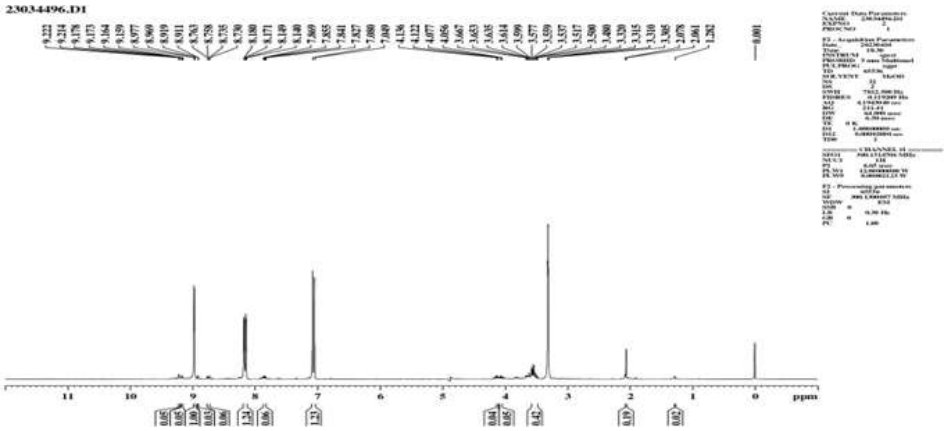

Fig.18. NMR of D-1

The ^{1}H NMR spectrum of quinoline was recorded, and the chemical shifts (δ, ppm) along with their multiplicities are summarized below: ^{1}HNMR (δ,ppm): 8.763 (1H, t, H-2), 8.730 (1H, t, H-4), 7.855 (1H, s, H-7), 7.827 (1H, t, H-3), 7.049 (1H, d, H-5).The downfield signal observed at δ 8.763 ppm (triplet) is assigned to H-2, which is significantly deshielded due to its proximity to the electronegative nitrogen atom of the quinoline ring. Similarly, the signal at δ 8.730 ppm (triplet) corresponds to H-4, influenced by the aromatic ring current and heteroatom effect. The proton at H-3 appears at δ 7.827 ppm as a triplet, indicating coupling with adjacent protons in the aromatic system. A distinct singlet at δ 7.855 ppm is assigned to H-7, suggesting isolated positioning with minimal coupling interactions. The doublet at δ 7.049 ppm corresponds to H-5, showing typical ortho-coupling with neighboring aromatic protons. Positions H-6 and H-8 do not show signals, which may be due to substitution, overlap, or absence in the analyzed structure. Overall, the ^{1}H NMR spectral data are consistent with the expected proton environment of the quinoline framework, confirming the structural integrity and aromatic nature of the compound.

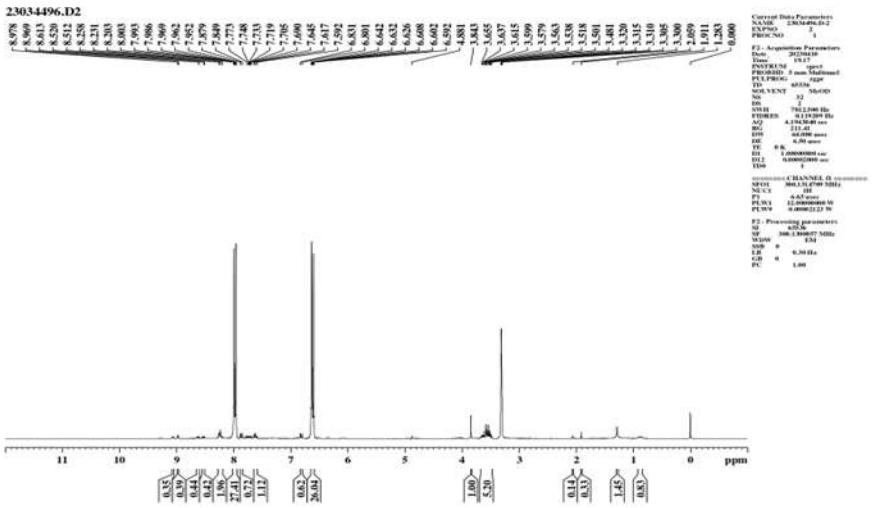

Fig.19. NMR of D-2

The ^{1}H NMR spectrum of the quinoline derivative was recorded, and the chemical shifts (δ, ppm) along with their multiplicities are summarized below: ^{1}HNMR (δ,ppm):8.763 (1H, t, H-2), 8.730 (1H, t, H-4), 8.003 (1H, d, H-8), 7.855 (1H, s, H-7), 7.827 (1H, t, H-3), 7.592 (1H, d, H-5).The most downfield signal at δ 8.763 ppm (triplet) is assigned to H-2, which is strongly deshielded due to the proximity of the ring nitrogen atom. The signal at δ 8.730 ppm (triplet) corresponds to H-4, influenced by both the heteroatom and aromatic ring current. The doublet at δ 8.003 ppm is attributed to H-8, indicating ortho-coupling with adjacent proton(s), while the singlet at δ 7.855 ppm corresponds to H-7, suggesting minimal or no coupling interactions due to its relative position. The signal at δ 7.827 ppm (triplet) is assigned to H-3, arising from coupling with neighboring protons. The doublet at δ 7.592 ppm corresponds to H-5, showing typical ortho-coupling behavior in the aromatic system. The absence of a signal for H-6 suggests substitution at this position or signal overlap, which is consistent with substituted quinoline derivatives. Overall, the ^{1}H NMR spectral data are consistent with the proposed quinoline framework and substitution pattern, confirming the structural integrity of the compound.

Mass Analysis

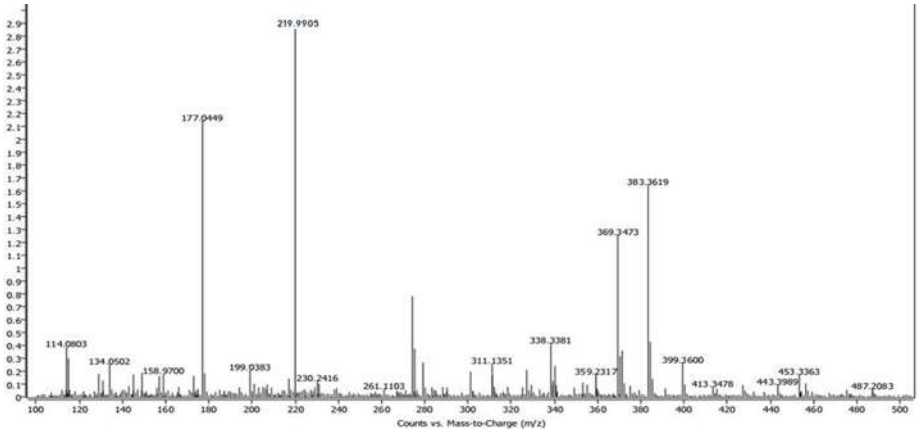

Fig.20. Mass spectrum of D-1

The mass spectrum of compound D-1 (6,8-dinitroquinoline) confirmed its molecular weight and supported the proposed structure. The spectrum exhibited a prominent molecular ion peak at m/z 219.9905, corresponding to the $[M]^+$ ion, which represents the intact molecule.This observed molecular ion peak is in close agreement with the theoretical molecular mass (m/z 219.15), thereby confirming the molecular formula and successful synthesis of the compound. The slight difference between observed and calculated values may be attributed to instrumental calibration and resolution factors.In addition to the molecular ion peak, several fragment ion peaks were observed, which provide valuable structural information. These fragments arise due to the cleavage of the quinoline ring system and loss of functional groups such as $–NO_2$, which is characteristic for nitro-substituted aromatic compounds. Such fragmentation patterns further support the presence and position of nitro substituents at the 6 and 8 positions of the quinoline nucleus.Overall, the mass spectral data strongly corroborate the proposed structure of compound D-1, confirming both its molecular weight and structural integrity.

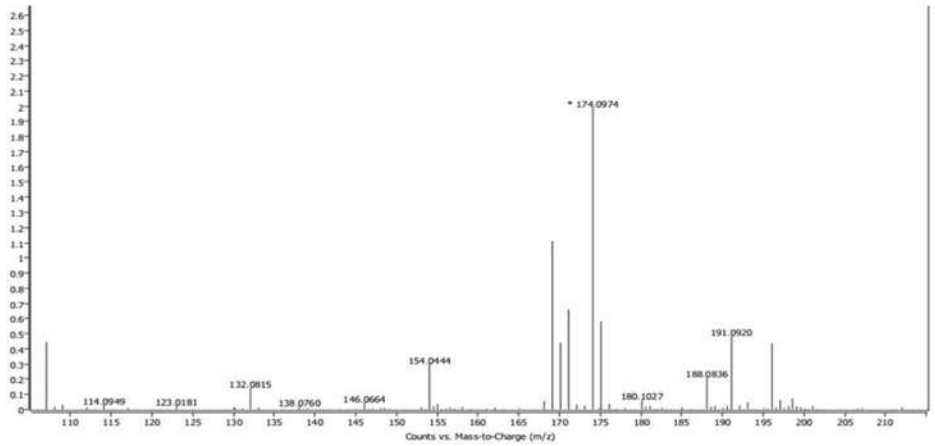

Fig.21. Mass spectrum of D-2

The mass spectrum of compound D-2 (6-nitroquinoline) confirmed its molecular weight and supported the proposed structure. The spectrum displayed a distinct molecular ion peak at m/z 174.0974, corresponding to the $[M]^+$ ion, which represents the intact molecule. The observed molecular ion peak is in close agreement with the theoretical molecular mass (m/z 174.15), thereby confirming the molecular formula and successful synthesis of the compound. The minor deviation between the experimental and calculated values can be attributed to instrumental calibration and measurement conditions. Additionally, the presence of fragment ion peaks provides further structural insights. These fragments are typically formed due to cleavage within the quinoline ring system and the loss of the nitro group ($–NO_2$), which is a common fragmentation pathway for nitro-substituted aromatic compounds. Such fragmentation behavior further supports the presence of the nitro substituent at the 6-position of the quinoline nucleus. Overall, the mass spectral data are consistent with the proposed structure of compound D-2, confirming both its molecular weight and structural integrity.

3.3 Pharmacological Evaluation

3.3.1 Actophotometer Model

TABLE.7. Actophotometer study

Sr.No.	Days	Control (Sec)	Standard (Diazepam) (Sec)	D-1 (Sec)	D-2 (Sec)
1	1	319.5 ± 0.7071	14.5 ± 0.7071	30.5 ± 0.7071	30.5 ± 0.7071
2	2	322.0 ± 1.4142	15.5 ± 0.7071	29.5 ± 0.7071	32.0 ± 2.8284
3	3	310.0 ± 14.1421	13.5 ± 0.7071	30.0 ± 1.4142	30.0 ± 1.4142
4	4	315.0 ± 0.7071	15.0 ± 1.4142	27.0 ± 2.8284	26.5 ± 0.7071

Effect of synthesized quinoline derivatives (D-1 and D-2) on sleeping time in experimental models compared with control and standard (Diazepam). Values are expressed as mean ± SD (n = 3).The results indicate that both D-1 and D-2 significantly reduced sleeping time compared to the control group, demonstrating central nervous system (CNS) depressant activity. However, their effects were less pronounced than the standard drug Diazepam, which showed the maximum reduction. Among the test compounds, D-2 exhibited slightly higher variability, while D-1 showed more consistent activity across all days.

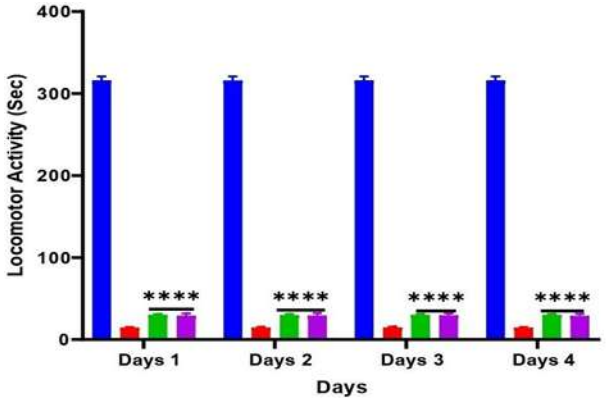

Fig.22. Effect on Locomotor Activities

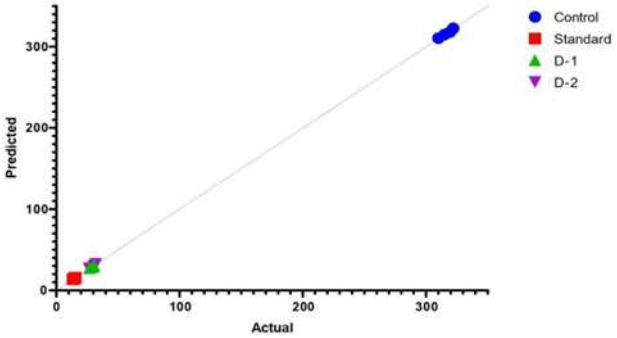

Fig.23. Nomal QQ plot for APM

The effect of the synthesized quinoline derivatives on locomotor activity was evaluated using an actophotometer model. The results are expressed as mean ± standard deviation (SD). The locomotor activity of the test compounds (D-1 and D-2) was compared with that of the standard drug Diazepam. Statistical analysis was performed using GraphPad Prism 9.0.1 software, followed by two-way ANOVA. A value of $p \leq 0.0001$ (****) was considered statistically highly significant. Both D-1 and D-2 exhibited a statistically significant reduction in locomotor activity compared to the standard drug, indicating pronounced central nervous system (CNS) depressant activity.

3.3.2 Elevated Plus Maze (EPM) Model

The anxiolytic activity of the synthesized compounds was evaluated using the Elevated Plus Maze (EPM) model**.** The behavioral parameters assessed included the number of entries into open and closed arms as well as the time spent in open and closed arms**.** Prior to experimentation, animals were acclimatized to the experimental conditions. Each animal was brought into the test room and allowed to remain in its home cage for 45–60 minutes to recover from handling stress. The maze apparatus was thoroughly cleaned with 70% ethanol before each trial to eliminate residual odors and ensure uniform testing conditions. During the experiment, video recording was initiated, and each mouse was placed at the center of the maze facing one of the open arms. Care was taken to maintain minimal disturbance; the observer remained out of the animal's sight and at a sufficient distance, and unnecessary movements or noise were strictly avoided throughout the session.

TABLE.8. Actophotometer study

Sr.No.	Groups	No. of Entries in Open Arm	No. of Entries in Closed Arm	Time Spent in Open Arm (Sec)	Time Spent in Closed Arm (Sec)
1	Control	14.50 ± 0.7071	4.50 ± 0.7071	129.50 ± 0.7071	119.50 ± 0.7071
2	Standard (Diazepam)	8.00 ± 1.4142	13.50 ± 0.7071	9.50 ± 0.7071	274.00 ± 1.4142
3	D-1	10.50 ± 0.7071	14.50 ± 0.7071	10.50 ± 0.7071	188.50 ± 0.7071
5	D-2	8.50 ± 2.1212	15.00 ± 0.7071	11.50 ± 0.7071	186.50 ± 2.1212

Effect of synthesized quinoline derivatives (D-1 and D-2) on elevated plus maze (EPM) parameters, including number of entries and time spent in open and closed arms. Values are expressed as mean ± SD (n = 3). The results indicate that both D-1 and D-2 altered the

exploratory behavior of animals in the EPM model. Compared to the control group, treated groups showed reduced open arm activity and increased time in closed arms, suggesting central nervous system depressant and anxiolytic-like effects. The standard drug Diazepam exhibited the most pronounced effect, while D-1 and D-2 showed moderate activity, supporting their potential pharmacological relevance.

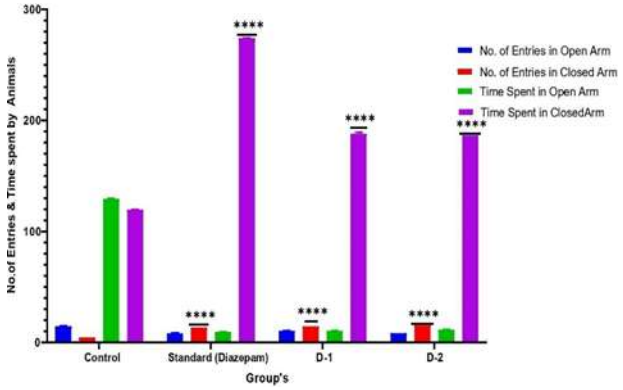

Fig.24. Effect of Derivatives on Animal Behaviour

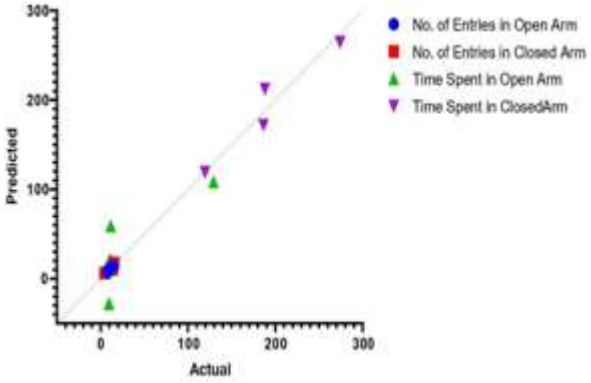

Fig.25. Nomal QQ plot For EPM

The effect of the synthesized quinoline derivatives on animal behavior was evaluated using the Elevated Plus Maze (EPM) model. The results are expressed as mean ± standard deviation (SD). The behavioral responses of the test compounds (D-1 and D-2) were compared with those of the standard drug Diazepam. Statistical analysis was performed using GraphPad Prism 9.0.1 software, followed by two-way ANOVA. A value of $p \leq 0.0001$ (****) was considered statistically highly significant.Both D-1 and D-2 demonstrated statistically significant effects compared to the standard drug, indicating notable influence on behavioral parameters in the EPM model, suggestive of central nervous system (CNS) activity.

4. CONCLUSION

A series of quinoline derivatives were successfully synthesized and evaluated for their CNS depressant activity. The microwave-assisted synthesis method proved to be superior to conventional methods in terms of reduced reaction time and higher yield.Molecular docking studies revealed that all designed compounds exhibited favorable binding affinity toward the $GABA_A$ receptor (PDB ID: 1J36) compared to the standard drug Diazepam. Among them, compounds D-1 and D-2 showed the highest binding affinities, indicating strong potential as CNS depressant agents. The synthesized compounds were characterized using FTIR, ^1H NMR, and mass spectrometry, confirming their structural integrity. Additionally, ADME studies demonstrated good drug-likeness with no violations of Lipinski, Ghose, and PAINS filters, while toxicity predictions indicated a generally safe profile. Pharmacological evaluation using actophotometer and elevated plus maze (EPM) models showed that D-1 and D-2 exhibited significant CNS depressant activity, comparable to the standard drug. Overall, based on molecular docking, ADMET profiling, toxicity assessment, and in vivo pharmacological studies, compounds D-1 (6,8-dinitroquinoline) and D-2 (6-nitroquinoline) were identified as the most promising CNS depressant candidates, warranting further investigation.

ACKNOWLEDGEMENT

The authors express their sincere gratitude to the management and faculty of the National College of Pharmacy, Nagpur, India for providing the

necessary facilities, infrastructure, and constant support to carry out this research work successfully. We are highly thankful to Dr. Ravee Kalsait and Dr. Dinesh Kawade for their valuable guidance, encouragement, and insightful suggestions throughout the course of this study. The authors also acknowledge the support of the Department of Chemistry, Priyadarshini J. L. College of Pharmacy, Hingna, Nagpur, for providing technical assistance and laboratory resources.

CONFLICT OF INTEREST

The authors declare that there is no conflict of interest regarding the publication of this research work. The study was conducted in the absence of any commercial or financial relationships that could be construed as a potential conflict of interest.

REFERENCES

1. Siddharth, Salahuddin, Siddhant, et al. “Ludwig Knorr’s Synthesis: Advances in Heterocyclic Synthesis of Quinoline, Quinolone, Pyrazole, and Pyrrole Derivatives.” Synthetic Communications 56, no.52026): 337–64.
2. Douara, Bachir, Marwa Manachou, Naima Merabet, Salima Boughdiri, and Lotfi Belkhiri. “Experimental and Theoretical Study of Quinoline Derivatives Obtained by Slight Modifications of the Standard Skraup Reaction.” Journal of Molecular Structure 1193 (October 2019): 416–28..
3. Saggadi, Hanen, Denis Luart, Nicolas Thiebault, Isabelle Polaert, Lionel Estel, and Christophe Len. “Toward the Synthesis of 6-Hydroxyquinoline Starting from Glycerol via Improved Microwave-Assisted Modified Skraup Reaction.” Catalysis Communications 44 (January 2014): 15–18.
4. Vallat, Brinda. “BPS2026 – RCSB Protein Data Bank: Delivering Integrative Structures alongside Experimental Structures and Computed Structure Models.” Biophysical Journal 125, no. 4 (2026): 263a.
5. Yagoo, Alex, M. C. John Milton, Jelin Vilvest, and Antony Stalin. “In Silico Molecular Docking Analysis on Acetylcholinesterase (AChE) Inhibition Activity on Aedes Aegypti and Culex Quinquefasciatus by β-Isocostic Acid.” Journal of Asia-Pacific Entomology 28, no. 3 (2025): 102433.
6. Kurnia, Dikdik, Sefren Geiner Tumilaar, Devi Meliani, Dudi Dudi, and Diding Latipudin. “Integrated Docking, ADMET, and Molecular Dynamics Study of Red Betel (Piper Crocatum) Compounds against SARS-CoV-2 Targets.” Phytomedicine Plus 6, no. 2 (2026): 100977.
7. Loganathan, Velmurugan, Idhayadhulla Akbar, Anis Ahamed, et al. “Synthesis, Antimicrobial and Cytotoxic Activities of Tetrazole N-Mannich Base Derivatives: Investigation of DFT Calculation, Molecular Docking, and Swiss ADME Studies.” Journal of Molecular Structure 1300 (March 2024): 137239.
8. Tasqeeruddin, Syed, Yahya I. Asiri, and Syeda Shaheen. “ NH4 CL /Zn Powder: An Efficient, Chemoselective Reducing Catalyst for the Microwave-assisted Synthesis of 2,3-disubstituted Quinolines via Tandem Knoevenagel Condensation.” Journal of Heterocyclic Chemistry 58, no. 2 (2021): 630–35.
9. Shrivastava, Anurag, and Rama Sushil. “Determination of Melting Point of Chemical Substances Using Image Differencing Method:” International Journal of Software Innovation 10, no. 1 (2022): 1–10.

10. Abe, Akira, Vania Hinkovska-Galcheva, and James A. Shayman. "Assessment of Bis(Monoacylglycerol)Phosphate Isomers by Thin Layer Chromatography Using a Modified Solvent System." Biochemistry and Biophysics Reports 44 (December 2025): 102303.
11. Khan, Mohammad Mansoob. "UV-Visible Spectroscopy and Diffuse Reflectance Spectroscopy." In Photocatalysts: Synthesis and Characterization Methods. Elsevier, 2025.
12. Dalyan, Eda, Çağrı Çavdaroğlu, Banu Özen, and Şükrü Güleç. "FTIR Spectroscopy Coupled with Chemometrics for Evaluating Functional Food Efficacy in an in Vitro Model of Iron Deficiency Anemia." Food Chemistry 506 (March 2026): 148196.
13. Powers, Robert, Erik R. Andersson, Amanda L. Bayless, et al. "Best Practices in NMR Metabolomics: Current State." TrAC Trends in Analytical Chemistry 171 (February 2024): 117478.
14. Thoren, Katie L. "Blood-Based MRD Testing in Multiple Myeloma: Update on Mass Spectrometry Methods for Detecting the Monoclonal Immunoglobulin." Seminars in Hematology, March06, S003719632600020X.
15. Chavinskaia, L., A. Boudon, S. Lemosquet, et al. "Opinion Paper: Working on Alternative Methods in Experimental Animal Sciences. Experience from the Case of Fistulated Ruminants." Animal, March 2026, 101799.
16. More, Nikhil, and Angel Godad. "Phenethyl Isothiocynate Attenuates Parkinson's Disease and Improves Performance in Hanging Wire, Rotarod and Actophotometer Test & Dopamine Levels in Rats via Inhibiting HDAC-1." Brain Disorders 17 (March 2025): 100183.
17. Andreatini, Roberto, and JoséR. Leite. "The Effect of Corticosterone in Rats Submitted to the Elevated Plus-Maze and to to Pentylenetetrazol-Induced Convulsions." Progress in Neuro-Psychopharmacology and Biological Psychiatry 18, no. 8 (1994): 1333–47.

HOW TO CITE: Jitendra Bhalavi, Dr. Ravi Kalsait, Dr. Dinesh Kawade, Green Synthesis and Evaluation of Quinoline-Based CNS Depressants, Int. J. of Pharm. Sci., 2026, Vol 4, Issue 5, 1213-1232. https://doi.org/10.5281/zenodo.20055585